NJC

PAPER

View Article Online
View Journal

Cite this: DOI: 10.1039/c7nj01656e

Development of pyridine based *o*-aminophenolate zinc complexes as structurally tunable catalysts for CO_2 fixation into cyclic carbonates†

Z. Alaji, [a] E. Safaei *[b] and A. Wojtczak[c]

Received 13th May 2017,
Accepted 28th July 2017

DOI: 10.1039/c7nj01656e

rsc.li/njc

Zinc complexes of $ZnL^{APIP}X$ (L = 2,4-di-*tert*-butyl-6-(((*E*)-2-(((*E*)-pyridin-2-lmethylene)amino)benzylidene)-amino)phenol) bearing different axial ligands (X = OAc, Cl, Br, I) have been successfully synthesized and characterized. It is evident from X-ray crystallography analysis that $ZnL^{APIP}X$ exists as a distorted square-pyramid in which Zn^{II} is coordinated by an *o*-aminophenolate-based ligand and an X moiety in the axial position. These easily synthesized complexes have been shown to perform as effective catalysts for the coupling of epoxides and carbon dioxide to generate cyclic carbonates. Their axial ligand was found to play an important role in enhancing their catalytic activity. The $ZnL^{APIP}I$ complex represents a versatile bifunctional catalyst due to the synergistic effect of both an electrophilic zinc ion and a nucleophilic iodide in one molecule to achieve a high-yield of cyclic carbonates, while $ZnL^{APIP}OAc$ in cooperation with a co-catalyst affords a productive system for this coupling reaction. The effects of reaction variables such as temperature, time and pressure were systematically investigated. This solvent free route is relevant to the context of green chemistry as it provides an atom-efficient protocol for the conversion of CO_2 into valuable cyclic carbonates.

Introduction

The expected global increase in CO_2 emissions from coal-fired power plants demands more sustainable methods of carbon dioxide capture, storage, and utilization.[1–5] In nature, large-scale capture and storage are achieved by conversion of CO_2 to carbonates by a series of cascade reactions carried out by metalloenzymes.[6] In particular, the zinc metalloenzyme carbonic anhydrase, fulfilling the requirement of an excellent catalyst for reversible hydration of CO_2 into carbonate with a high turnover number of 10^7, plays an important role in various biological systems.[7,8] The use of carbon dioxide as a safe, inexpensive and abundant C_1 feedstock for the synthesis of useful chemicals and as a fluid in numerous applications can contribute to a sustainable chemical industry and concomitantly reduce CO_2 emissions into the atmosphere.[1,6,9,10] In this regard, the atom efficient synthesis of either valuable polymeric carbonates or cyclic carbonates through the cycloaddition of CO_2 to epoxide is of great importance in industry (Scheme 1).[1,11–14]

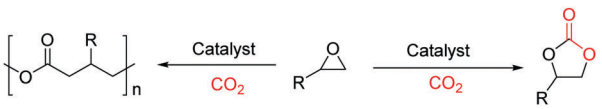

Scheme 1 Synthesis of polymeric or cyclic carbonates from CO_2 and epoxides.

Cyclic carbonates are valuable synthetic targets because of their relevant properties.[15] High molecular dipole moments, high dielectric constants and high boiling temperatures make cyclic carbonates suitable as highly green polar aprotic solvents[16–21] and as ion-carriers for lithium-ion batteries.[22,23] In addition, they find applications for the production of additives in lubricants, as precursors for pharmaceutical intermediates in drugs,[3,24] and more specifically as monomers for the preparation of polyurethanes,[25] polycarbonates,[26] and polyglycerol,[27] and also as precursors for diastereo selective formation of diols.[28,29]

In addition, since CO_2 is such an inert molecule, these processes are significantly energy demanding.[30] Therefore, the reactivity may be greatly enhanced by the judicious choice of catalysts. Typically, for the promotion of CO_2/epoxide coupling, binary catalytic systems including a Lewis acid and a nucleophile are employed. The Lewis acid activates the epoxide towards ring opening resulting from the attack of the nucleophile to the less substituted carbon atom. This reaction is followed by CO_2 insertion which leads to ring closure, *via* a backbiting mechanism

[a] *Institute for Advanced Studies in Basic Sciences (IASBS), 45137-66731, Zanjan, Iran*
[b] *Department of Chemistry, College of Sciences, Shiraz University, 71454, Shiraz, Iran. E-mail: e.safaei@shirazu.ac.ir*
[c] *Faculty of Chemistry, Nicolaus Copernicus University, 87-100 Torun, Poland*

† Electronic supplementary information (ESI) available: The characterization data, and copies of ^1H, ^{13}C NMR spectra, and MALDI-MS spectra. CCDC 1497259, 1497260 and 1497261. For crystallographic data in CIF or other electronic format see DOI: 10.1039/c7nj01656e

producing the cyclic carbonate and regenerating the nucleophile.[31] In this regard, metal complexes as catalysts (Lewis acid) in combination with auxiliary nucleophiles play a pivotal role in activation and utilization of CO_2 as a source of chemical carbon.[32] Successful examples of metal complexes of magnesium,[9,33] aluminium,[28,34–40] chromium,[41,42] cobalt,[43] zinc,[44] and iron[45–47] coupled mainly with porphyrins,[48–50] salen[39,51–55] and salophen[56–59] have been developed. Among these, Zn-based complexes exhibit some advantages such as low toxicity, low price, and high stability towards oxidation.[60,61] Recently, bifunctional catalysts of metal salen complexes, organocatalysts,[62–65] and ionic liquids[66–69] presented high activity and selectivity. Several Co(salen)X,[70–72] Al(salen)Cl[2,59] and μ-oxo-bimetallic salen aluminium complexes[73,74] have been prepared which contain quaternary onium salts or quaternary phosphonium salts[75] tethered to the salen ligand, thereby affording a single component catalyst. In bifunctional catalysts, it is unnecessary to use a co-catalyst, and also easy to explore the mechanism and reuse the catalyst.[35]

Despite these advancements, further improvements are still needed to synthesize versatile catalysts to achieve high catalytic activity both in terms of control and selectivity with binary and bifunctional systems.

We were interested in developing discrete complexes with a nucleophilic axial X group promoting the catalytic activity in the absence of a co-catalyst. This accomplishment is achieved by the subtle tuning of the axial ligand into an iodide anion to offer a robust zinc complex of the *o*-aminophenolate ligand as a bifunctional catalyst for this coupling reaction. Metal complexes of *o*-aminophenolate ligands bearing various substituents are an important class of compounds, because they allow the tuning of steric and electronic properties of the catalyst, thus promoting a variety of catalytic reactions.[76–80] In this article, we report one pot and easy synthesis of pyridine based *o*-aminophenolate zinc complexes with different axial ligands (OAc, Cl, Br, I) (Scheme 2). The catalytic activity of these complexes for the coupling of epoxides and carbon dioxide to produce cyclic carbonates in the absence of organic solvents is evaluated. The effect of the axial ligand on the catalytic activity of the different complexes for the coupling of epoxides and carbon dioxide has been examined in the presence of a co-catalyst.[18,81–84]

Results and discussion

X-Ray crystallography of $ZnL^{APIP}X$ (X = OAc, Br, I) complexes

The asymmetric part of all structures is constituted by a molecular complex [$Zn(L^{APIP})(X)$], where X denotes acetate, Br or I anions (Fig. 1). Complexes $ZnL^{APIP}OAc$ and $ZnL^{APIP}Br$ crystallize in the triclinic space group $P\bar{1}$, while $ZnL^{APIP}I$ crystallizes in the monoclinic $P2_1/n$ space group. The diffraction experiment and the structure refinement data of $ZnL^{APIP}X$ (X = OAc, Br, I) are presented in Table 1. A water molecule with the occupancy set to 50% is found in complex $ZnL^{APIP}OAc$. In all complexes, the coordination sphere of ZnN_3OX has a distorted square pyramid geometry. Selected bond lengths and angles are summarized in Table 2. The four-dentate L^{APIP} ligand coordinates in a square-planar manner and an anion X acts as a monodentate axial ligand. The overall shape of all molecules is a bowl formed by the L^{APIP} ligand with the central Zn(II) ion slightly shifted above the N_3O pyramid base towards the axially coordinated anion (0.631, 0.728 and 0.726 Å) for $ZnL^{APIP}X$ (X = OAc, Br, I) respectively. In the coordination N_3O plane of all complexes, the Zn–O distances involving the L^{APIP} phenolate group are the shortest (Table 2). This value is a little larger than the Zn–O bond distance reported in Zn(salpyr) complexes.[58] In all complexes, the Zn–N bonds formed by N1 adjacent to the phenol moiety are shorter than those formed by pyridyl N3. While, the Zn–N2 bonds are the longest within the N_3O plane, which reflects the rigidity of L^{APIP} acting as a four-dentate ligand. In $ZnL^{APIP}OAc$, the Zn–O2 bond length formed by acetate is 1.991(4) Å which is slightly longer than the Zn–O1 bond length of phenolate (1.977(3) Å).

In $ZnL^{APIP}Br$, the significant effect of the bulk imposed by the Br ligand is clearly visible. The dihedral angles in $ZnL^{APIP}Br$ are larger than those found in $ZnL^{APIP}OAc$. In $ZnL^{APIP}I$, the corresponding angles are almost identical to those in $ZnL^{APIP}OAc$. An analogous architecture is also found for the $ZnL^{APIP}Cl$ complex not reported here due to its low quality structure (Fig. S1, ESI†).

Catalytic activity of $ZnL^{APIP}X$ (X = OAc, Cl, Br, I)

The conversion of styrene oxide with CO_2 to produce styrene carbonate was chosen as a typical reaction to examine the catalytic activity of the Zn-based catalysts (Scheme 3 and Table 3).

First, screening experiments were performed at 100 °C, with the initial CO_2 pressure of 1.0 MPa, for 4 h with 0.5 mol% catalyst loading of $ZnL^{APIP}X$ (X = OAc, Cl, Br and I) without any co-catalyst. Among the zinc-based catalysts, $ZnL^{APIP}I$ permitted an excellent yield of up to 94% of cyclic styrene carbonate **1b** (Table 3, entry 6).

In contrast, the catalysts containing bromide and chloride ligands showed a dramatic decrease in the yield of styrene carbonate **1b** in 4 hours (Table 3, entries 2 and 4); while they afforded moderate yields of 70% and 45% at a long reaction

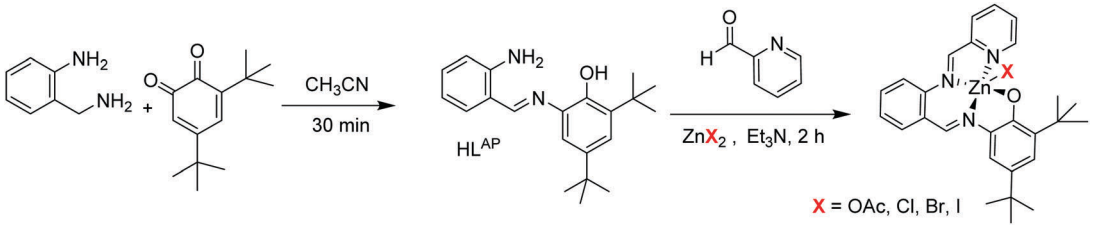

Scheme 2 One-pot synthesis of $ZnL^{APIP}X$ (X = OAc, Cl, Br, I) complexes.

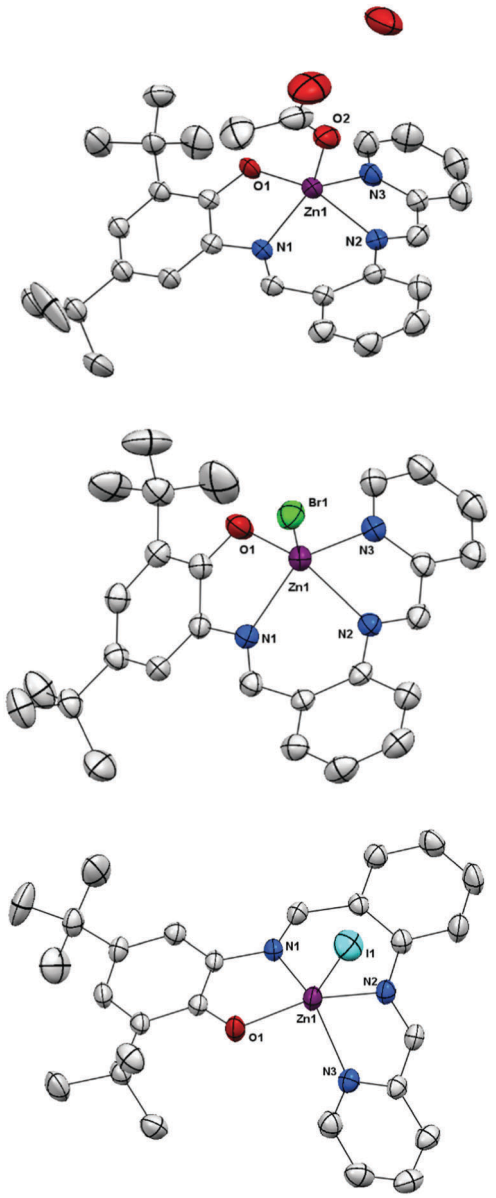

Fig. 1 Molecular structure of $Zn^{LAPIP}OAc$, $ZnL^{APIP}Br$, and $Zn^{LAPIP}I$. Hydrogen atoms have been omitted for clarity. Thermal ellipsoids are set at 50% probability.

time of 12 h (Table 3, entries 3 and 5). For the bifunctional Zn-based catalyst, the yield of **1b** increased with the order of the atomic number of the halide $Cl^- < Br^- < I^-$. A change in the axial anion to the more nucleophilic iodide increases the styrene carbonate formation, while the less-nucleophilic acetate nearly caused the loss of catalyst activity at a 4 h reaction time. Comparison of the structures reveals that the length of the axial Zn–X bond increases in the same trend (Table 2). Additionally, in $ZnL^{APIP}Br$ and $ZnL^{APIP}I$ complexes, the axial ligand has no intramolecular non-bonding interactions with the L^{APIP} ligand. On the contrary, in $ZnL^{APIP}OAc$ the C29 methyl group of acetate forms additional interactions with atoms in the Zn1–O1–C1–C6–N1 chelate ring. Most likely, the longest bond distance of Zn–I in the $ZnL^{APIP}I$ molecule, as well as it having no intramolecular interactions, makes the iodide anion more prone to leave the Zn center and act as a nucleophile. Reversible interactions between the halide anions and the Zn ions are a prerequisite for catalytic activity, because the halide is involved in nucleophilic ring-opening of the epoxide substrate and Zn–X dissociation also allows for coordination of the epoxide to the Lewis acidic Zn center. The non-polar nature of the *tert*-butyl groups was important to ensure that the catalyst dissolved in the epoxide and showed high levels of catalytic activity.[85,86] We also examined the temperature effect on $ZnL^{APIP}I$ performance at 70 °C. It obtained a poor yield of 22% styrene carbonate (Table 3, entry 7), implying that activation of the axial ligand to act as a nucleophile probably requires a high temperature of 100 °C.[56,66,87,88] Performing the reaction using ZnI_2 under the same reaction conditions of $ZnL^{APIP}I$ at 100 °C also gave a very poor yield of 3% (Table 3, entry 8).

TBAI was also examined and afforded a yield of 70% under the same reaction conditions (Table 3, entry 9). It is worth noting that the $ZnL^{APIP}I$ catalyst was recovered by isolating the formed cyclic carbonate and drying the catalyst *in vacuo*. It was reused for the subsequent run without significant loss in its catalytic activity (Table 3, entry 10).

Rieger and co-workers presented the tetraamine–iron complex as a one component catalyst comprising an easily modified ligand motif with iron as the metal centre. This iron catalyst was active in cyclic carbonate synthesis through the coupling of CO_2 with propylene oxide using a catalyst loading of 1.5 mol% at a CO_2 pressure of 1.5 MPa at 2 h.[87] Recently Kleij and co-workers reported that a tetraoxo bis-Zn (salphen) supramolecular host can bind various divalent metal salts, thereby providing access to tri-nuclear bifunctional systems that incorporate both Lewis acid sites and dynamically bound nucleophilic anions. This catalytic system was capable of catalyzing the coupling reaction of terminal epoxides with CO_2 using high amounts of catalyst loading (2.5 mol%) at a relatively long reaction time of 18 h.[88] In comparison with bifuntional catalytic systems in which the axial ligand performs as a nucleophile, our catalysis system ($ZnL^{APIP}I$) could afford excellent results with a broad substrate scope tolerance using a low amount of catalyst loading (0.5 mol%) at 4 h. This result indicates the significant effect of the *o*-aminophenolate-iminopyridine ligand, which facilitates the solubility as well as the leaving ability of the iodide anion in the $ZnL^{APIP}I$ complex. It has been demonstrated that the Lewis acidic properties of the metal can be tuned by the electronic properties of the ligand, which may influence the reactivity and catalytic behavior of the complex.[89,90]

On the basis of the catalytic activity of $ZnL^{APIP}X$ (X = OAc, Cl, Br, and I), the coordination–insertion mechanism can be inferred.[91] The metal complex initiates the coupling reaction by coordinating the epoxide followed by the attack of a nucleophilic group (nucleophilic axial anion or added co-catalyst), leading to epoxide ring-opening and formation of a metal-bound alkoxide. CO_2 insertion provides a metal-bound carboxylate, followed by the production of cyclic carbonate *via* a backbiting pathway.

The proposed mechanism including the replacement of the halide ligand by the epoxide substrate could also be approved

Table 1 Crystal data and structure refinement for $ZnL^{APIP}X$ (X = OAc, Br, I)

Identification code	$ZnL^{APIP}OAc$	$ZnL^{APIP}Br$	$ZnL^{APIP}I$
Empirical formula	$C_{29}H_{34}N_3O_{3.50}Zn$	$C_{27}H_{30}BrN_3OZn$	$C_{27}H_{30}IN_3OZn$
Formula weight	545.96	557.82	604.81
Temperature, K	293(2)	293(2)	293(2)
Wavelength, Å	0.71073	0.71073	0.71073
Crystal system, space group	Triclinic, $P\bar{1}$	Triclinic, $P\bar{1}$	Monoclinic, $P2_1/n$
Unit cell dimensions, Å, °	a = 10.1927(13)	a = 7.9476(3)	a = 13.7585(6)
	b = 10.2059(12)	b = 11.5809(5)	b = 12.5082(4)
	c = 14.7907(19)	c = 14.2737(6)	c = 15.7328(6)
	α = 94.834(10)	α = 83.054(4)	
	β = 98.779(11)	β = 76.725(4)	β = 110.107(4)
	γ = 114.583(12)	γ = 89.507(3)	
Volume, Å^3	1364.0(3)	1269.02(10)	2542.49(18)
Z, calculated density, mg m^{-3}	2, 1.329	2, 1.460	4, 1.580
Absorption coefficient, mm^{-1}	0.937	2.566	2.204
F(000)	574	572	1216
Crystal size, mm	0.53 × 0.31 × 0.17	0.661 × 0.326 × 0.186	0.599 × 0.229 × 0.062
Reflections collected/unique	8580/5709 [R(int) = 0.0566]	8731/5668 [R(int) = 0.0384]	17 638/5858 [R(int) = 0.0313]
Absorption correction	Analytical	Analytical	Analytical
Max. and min. transmission	0.8586 and 0.6369	0.686286 and 0.338022	0.869034 and 0.492954
Data/restraints/parameters	5709/0/334	5668/0/298	5858/0/298
Goodness-of-fit on F^2	1.069	0.882	0.918
Final R indices [$I > 2\sigma(I)$]	R_1 = 0.0611, wR_2 = 0.1653	R_1 = 0.0375, wR_2 = 0.0796	R_1 = 0.0284, wR_2 = 0.0569
R indices (all data)	R_1 = 0.0851, wR_2 = 0.2129	R_1 = 0.0639, wR_2 = 0.0859	R_1 = 0.0493, wR_2 = 0.0601

Table 2 Selected bond lengths [Å] and angles [°] for the $ZnL^{APIP}X$ (X = OAc, Br, I) complexes

	$ZnL^{APIP}OAc$	$ZnL^{APIP}Br$	$ZnL^{APIP}I$
Zn1–O1	1.977(3)	1.960(2)	1.9616(14)
Zn1–N1	2.086(3)	2.106(2)	2.1164(18)
Zn1–N3	2.110(4)	2.121(2)	2.1257(19)
Zn1–N2	2.174(3)	2.170(2)	2.1621(18)
Zn1–O2	1.991(4)	—	—
Zn1–Br1	—	2.4002(4)	—
Zn1–I1	—	—	2.5765(3)
O1–Zn1–O2	111.90(13)	—	—
O2–Zn1–N1	117.07(14)	—	—
O2–Zn1–N3	105.44(15)	—	—
O2–Zn1–N2	94.73(13)	—	—
O1–Zn1–Br1	—	112.25(6)	—
N1–Zn1–Br1	—	111.95(6)	—
N3–Zn1–Br1	—	116.75(6)	—
N2–Zn1–Br1	—	99.24(6)	—
O1–Zn1–I1	—	—	114.73(5)
N1–Zn1–I1	—	—	117.60(5)
N3–Zn1–I1	—	—	106.81(5)
N2–Zn1–I1		—	101.16(5)

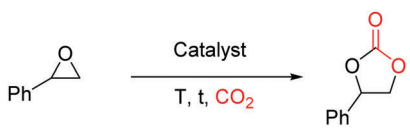

Scheme 3 Coupling reaction of styrene oxide and CO_2 to produce styrene carbonate.

by the structural data. That is, acetate is involved in a much more complexed network of intramolecular interactions, therefore it is not easy to be released from the coordination sphere. It may be hypothesized that with the increasing length of the axial Zn–X bond and more relaxed molecules, as found in complexes of $ZnL^{APIP}Br$ and $ZnL^{APIP}I$, the X ligand is more labile and can be easily substituted by the substrate, which seems to correlate with the catalytic activity data.

Table 3 Conversion of styrene epoxide and CO_2 into the corresponding styrene carbonate using $ZnL^{APIP}X$ (X = OAc, Cl, Br, I)

Entry[a]	Catalyst	T (°C)	Yield[b] (%)	Time (h)	TON[c]
1	$ZnL^{APIP}OAc$	100	5	4	10
2	$ZnL^{APIP}Cl$	100	10	4	20
3	$ZnL^{APIP}Cl$	100	45	12	90
4	$ZnL^{APIP}Br$	100	30	4	60
5	$ZnL^{APIP}Br$	100	70	12	140
6	**$ZnL^{APIP}I$**	**100**	**94**	**4**	**188**
7	$ZnL^{APIP}I$	70	22	4	44
8	ZnI_2	100	3	4	6
9	TBAI[d]	100	70	4	140
10	$ZnL^{APIP}I$[e]	100	90	4	180

[a] Solvent free-reaction conditions: styrene oxide (10 mmol, 1.140 mL), catalyst (0.5 mol%), $p(CO_2)$ = 1.0 MPa. [b] Selectivity for the cyclic carbonate product >99% in all entries (unless stated otherwise) determined by GC using biphenyl as the internal standard and GPC. [c] Turnover number (TON): mole of styrene carbonate per mole of catalyst. [d] Tetrabutylammonium iodide (TBAI). [e] Reused catalyst.

Substrate scope of $ZnL^{APIP}I$ catalytic activity

To explore the generality of $ZnL^{APIP}I$ as a bifunctional catalyst in the coupling reaction of epoxides and CO_2, the substrate scope was investigated with 0.5 mol% of this catalyst, and a CO_2 pressure of 1.0 MPa at 100 °C (Scheme 4). Different kinds of terminal epoxides were tolerated in this catalysis system. Alkyl, aryl-substituted and glycidol-derived ether and ester substrates were converted into the corresponding cyclic carbonates with excellent yields.

Epichlorohydrin, **8b**, was converted into **9b**, and a bis-epoxide substrate was also cleanly converted into its bis-carbonate product **11b** in good yield (80%).

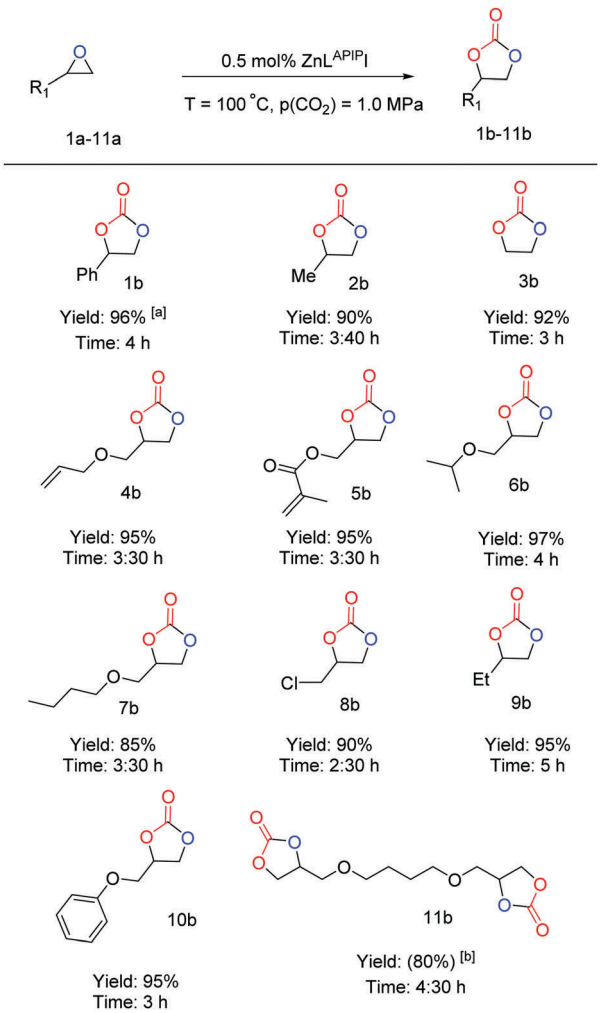

Scheme 4 Substrate scope for the synthesis of organic carbonates **1b–11b** using ZnL^{APIP}I. General conditions: epoxide (10 mmol), ZnL^{APIP}I (0.5 mol%), T = 100 °C, $p(CO_2)$ = 1.0 MPa. [a] GC yield using biphenyl as the internal standard. [b] Isolated yield obtained after column chromatography (only for this substrate). Selectivity for the cyclic carbonate product >99% in all examples determined by GC using biphenyl as the internal standard and ^{1}H NMR.

Catalytic activity of ZnL^{APIP}OAc

Given that the zinc complexes containing Br, Cl and acetate as axial ligands, similar to most of the metal complexes,[42,51,92] are not capable of efficient conversion of epoxides to the corresponding cyclic carbonates in the absence of a co-catalyst, we were motivated to employ ZnL^{APIP}OAc in combination with a co-catalyst as a binary catalyst. Werner pointed out that a nucleophilic species for the ring opening of the epoxide is essential. Furthermore, Lewis acidic homogeneous metal complexes accelerate the addition of CO_2 to epoxides, but there is only very low or even no catalytic activity if there is no nucleophile or co-catalyst.[62]

The first screening experiments were performed at 100 °C, with an initial CO_2 pressure of 1.0 MPa, for 2 h with 2 mol% catalyst loading in dichloromethane and acetonitrile, resulting in moderate and good yields of styrene carbonate, respectively (Table 4, entries 1 and 2). To afford an atom-economic and environmental friendly reaction, we examined solvent-free conditions as well.

Table 4 Conversion of styrene epoxide and CO_2 into the corresponding styrene carbonate catalyzed by ZnL^{APIP}OAc catalysts under various conditions

Entry[a]	Catalyst (mol%)	Co-catalyst (mol%)	T (°C)	$p(CO_2)$ (MPa)	Yield[b] (%)	Time (h)	TON[e]
1[c]	(2)	TBAB[f] (2)	100	1	70	2	35
2[d]	(2)	TBAB (2)	100	1	95	2	48
3	(1)	TBAB (2)	100	1	85	2	85
4	(1)	—	100	1	10	2	10
5	(2)	TBAB (2)	100	1	70	2	35
6	(0.5)	TBAB (2)	100	1	90	2	180
7	(0.2)	TBAB (2)	100	1	97	2	485
8	(0.1)	TBAB (1)	100	1	95	2	950
9	—	TBAB (1)	100	1	60	2	—
10	(0.1)	TBAB (0.5)	100	1	80	2	800
11	(0.1)	TBAB (0.1)	100	1	20	2	200
12	(0.1)	TBAB (1)	70	1	96	4	960
13	(0.1)	TBAB (1)	70	0.5	80	4	800
14	(0.1)	TBAB (1)	70	0.1	40	4	400
15	(0.1)	TBAI (1)	70	1	90	2	900
16	(0.1)	TBAB (1)	70	1	80	2	800
17	(0.1)	TBAC[g] (1)	70	1	82	2	820
18	(0.1)	DMAP[h] (1)	70	1	15	2	150
19	**(0.1)**	**TBAI (1)**	**70**	**1**	**97**	**3**	**970**
20	(0.05)	TBAI (0.5)	70	1	85	3	1700
21	—	TBAI (1)	70	1	50	2	—
22	—	TBAI (0.5)	70	1	30	3	—

[a] Solvent free-reaction conditions (unless otherwise stated): styrene oxide (10 mmol, 1.140 mL), catalyst, co-catalyst. Selectivity for the cyclic carbonate product >99% in all entries. [b] GC yield using biphenyl as the internal standard. [c] Reaction conditions: styrene oxide (2 mmol, 0.228 mL), catalyst (0.0218 g, 2 mol%), TBAB (0.0128 g, 2 mol%), $p(CO_2)$ = 1.0 MPa, 100 °C, CH_2Cl_2 (2 mL). [d] Reaction conditions styrene oxide (2 mmol, 0.228 mL), catalyst (0.0218 g, 2 mol%), TBAB (0.0128 g, 2 mol%), $p(CO_2)$ = 1.0 MPa, 100 °C, CH_3CN (2 mL). [e] Turnover number (TON): mole of styrene carbonate per mole of catalyst. [f] Tetrabutylammonium bromide (TBAB). [g] Tetrabutylammonium chloride (TBAC). [h] 4-Dimethylaminopyridine (DMAP).

To set a catalytic benchmark, different co-catalyst to catalyst ratios were tested in this coupling reaction. These catalytic tests showed some general trends with a number of promising results (Table 4, entries 3–11).

In our work, it was confirmed (Table 4, entry 8) that 0.1 mol% ZnL^{APIP}OAc catalyst in combination with 1 mol% tetrabutylammonium bromide (TBAB) afforded an excellent yield of 95% in 2 hours for the production of styrene carbonate **1b** with high selectivity. The low yield of product formation at a high catalyst loading amount (Table 4, entry 5) can be attributed to the poor solubility of the catalyst in styrene oxide.

Using ZnL^{APIP}OAc without a nucleophilic moiety showed a poor yield (Table 4, entry 4), and using TBAB or TBAI alone (Table 4, entries 9, 21 and 22), gave yields of 60%, 50% and 30% respectively. These experiments, in agreement with other reports elucidate the importance of a nucleophile for this catalytic activity.[52,92]

Regarding the investigated reaction parameters, temperature had the most decisive effect on the model reaction (Fig. 2).

So the effect of temperature was examined during 2 hours of reaction time. However, even at a temperature of 50 °C, a relatively good yield of 34% cyclic styrene carbonate **1b** was

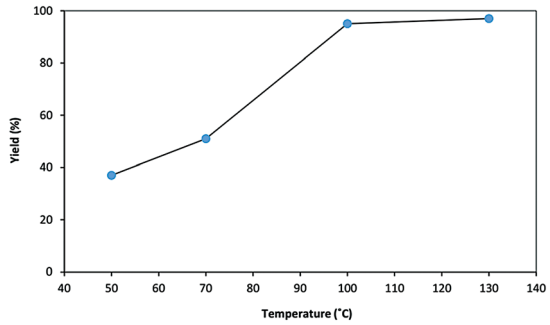

Fig. 2 Effect of the reaction temperature on the yield of styrene carbonate. Reaction conditions: styrene oxide (10 mmol, 1.140 mL), ZnL^{APIP}OAc (0.0055 g, 0.1 mol%), TBAB (0.0322 g, 1 mol%), $p(CO_2)$ = 1.0 MPa, time = 2 h.

observed. Moreover, at 70 °C, a moderate yield of 51% was obtained. The excellent yield of 95% was obtained at the temperature of 100 °C. Upon further raising the temperature to 130 °C, no significant enhancement in styrene carbonate production was observed. Having explored the temperature effect, it was also found that this coupling reaction at 70 °C at the extended time of 4 hours affords an excellent yield of 96% (Table 4, entry 12); thus, other experiments to determine the dependence of yield on carbon dioxide pressure and co-catalyst amount were performed at 70 °C. Darensbourg showed that the formation of the cyclic carbonate was thermodynamically favoured over the formation of the polycarbonate, as the kinetic product, which is favoured at lower temperatures.[41,84] Therefore we carried out GPC analysis for the reaction mixture of Table 4, entry 12, to get more information about the reaction content. It did not exhibit any polymer chain when the reaction was performed at a mild temperature of 70 °C (Fig. S2, ESI†).

Furthermore, the carbon dioxide pressure impact was investigated at 0.1 MPa, 0.5 MPa and 1.0 MPa (Table 4, entries 12–14). In the model reaction, even at a carbon dioxide pressure of 0.1 MPa, 40% of epoxide **1a** was converted into **1b** with no side product. Styrene carbonate **1b** was obtained in good yield for a CO_2 pressure of 0.5 MPa and it was enhanced to an excellent yield of 96% at a CO_2 pressure of 1.0 MPa. Considering the full conversion of **1a** and the high yield of cyclic carbonate **1b**, the CO_2 pressure of 1.0 MPa was chosen for further investigations. To clarify the significant effect of the co-catalyst, the reaction time was set to 2 h. Among the employed co-catalysts, DMAP exhibited a very poor effect on the model reaction conversion with a low yield (15%), while onium salts had a positive effect on styrene carbonate formation (Table 4, entries 15–18). TBAI gave the highest yield of 90% of **1b**, so it was selected for further studies. Full conversion of **1a** using TBAI is achieved in 3 h (Table 4, entry 19). Decreasing the amount of catalyst to 0.05 mol% and using TBAI as a co-catalyst yielded a very good turnover number of 1700 in 3 h (Table 4, entry 20). From parameter screening, the standard reaction conditions were defined as 70 °C, a CO_2 pressure of 1.0 MPa and a co-catalyst to catalyst ratio of 10.

To investigate the applicability of the ZnL^{APIP}OAc/TBAI system, the substrate scope was also examined (Scheme 5). It showed high efficiency for different substrates at conditions of

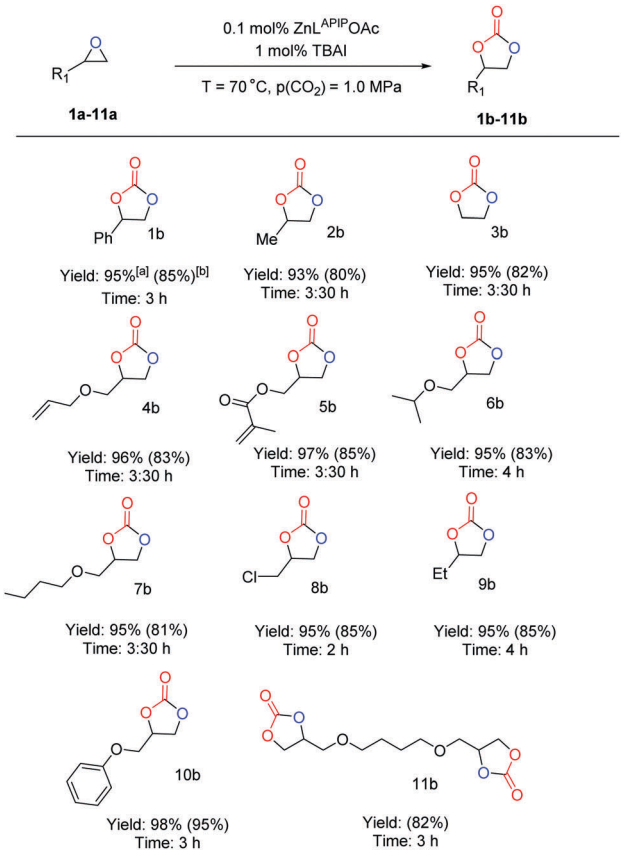

Scheme 5 Substrate scope for the synthesis of organic carbonates **1b–11b** using ZnL^{APIP}OAc/TBAI. General conditions: epoxide (10 mmol), ZnL^{APIP}OAc (0.1 mol%), NBu_4I (1 mol%), T = 70 °C, $p(CO_2)$ = 1.0 MPa. Selectivity towards the cyclic carbonate product was >99% determined by GC using biphenyl as the internal standard and ^{1}H NMR; in all cases the first number, [a] is GC yield using biphenyl as the internal standard and the second number in brackets, [b] is isolated yield obtained after column chromatography.

0.1 mol% ZnL^{APIP}OAc and 1 mol% TBAI at 70 °C. All products were isolated. The corresponding carbonates **4b** and **5b** are potential building blocks for homo- and copolymerization products with a cyclic carbonate unit in the backbone.[93] We isolated these products in yields of up to 85% under the reaction conditions. (In some cases, the effects arising from isolation through column purification resulted in lower isolated yields). A number of Zn-based binary catalytic systems for chemical fixation of CO_2 into cyclic carbonates have been developed.[44,57,60,94] For example, Klije *et al.* presented a highly active Zn(salphen) catalyst for production of organic carbonates in a green CO_2 medium in a solvent-free, CO_2-rich environment. They suggested that the solvent free condition provides an efficient interaction between CO_2 and the reagents improving the catalyst performance.[94] Very recently, Godard and co-workers reported zinc complexes containing pyrrolidine-based ligands as robust catalysts in the coupling of CO_2 with terminal and internal epoxides with TBAI as a co-catalyst. They demonstrated that the Zn complex with an N4 (pyrollidine) coordination environment exhibited a high turnover number of

Table 5 Conversion of cyclohexene epoxide and CO_2 into the corresponding cyclohexene carbonate under various conditions

Entry[a]	Catalyst (mol%)	Co-catalyst (mol%)	T (°C)	Yield[b] (%)	Sel.	TON[c]
1	$ZnL^{APIP}OAc$ (0.1)	TBAI (1)	70	45	>99	450
2	$ZnL^{APIP}OAc$ (0.1)	TBAI (1)	100	57	>99	570
3	$ZnL^{APIP}OAc$ (0.1)	TBAB (1)	100	74	>99	740
4	$ZnL^{APIP}OAc$ (0.2)	TBAB (2)	100	88	>99	440
5	$ZnL^{APIP}OAc$ (0.2)	TBAC (2)	100	59	>99	295
6	$ZnL^{APIP}I$ (0.5)	—	100	22	>90	44
7	$ZnL^{APIP}I$ (0.2)	TBAB (2)	70	60	>90	300
8	$ZnL^{APIP}I$ (0.2)	TBAB (2)	100	76	>90	380
9	$ZnL^{APIP}Br$ (0.2)	TBAB (2)	100	81	>95	405
10	$ZnL^{APIP}Cl$ (0.2)	TBAB (2)	100	90	>95	450
11	—	TBAB (2)	100	55	>85	—

[a] Solvent free-reaction conditions (unless otherwise stated): cyclohexene oxide (10 mmol, 1.0 mL), catalyst, co-catalyst, $p(CO_2)$ = 1.0 MPa; time = 10 h. [b] GC yield using biphenyl as the internal standard. Selectivity for the cyclic carbonate product determined by ^{1}H NMR and GPC. As confirmed by ^{1}H NMR, *cis*-cyclohexene carbonate was the only observed isomer. [c] Turnover number (TON): mole of styrene carbonate per mole of catalyst.

up to 1560 for styrene oxide (80 °C, 30 bar, 16 h). Compared to the reported catalytic systems, $ZnL^{APIP}OAc$/TBAI operates at a lower CO_2 pressure (10 bar), and 70 °C in a short reaction time of 3 h to obtain a good turnover number of 1700 for styrene oxide.

Non-terminal cyclohexene epoxide is often considered to be a challenging substrate to be converted to a cyclic carbonate. The steric hindrance of nucleophilic ring opening of the cyclohexene epoxide usually causes lower yields and, as a consequence, more drastic reaction conditions are required. Moreover, the structure of cyclic cyclohexene carbonate consists of a six-membered ring interconnected to a five-membered ring and is, therefore, geometrically strained. So, we studied the reaction of cyclohexene oxide catalysed by the new zinc complexes in detail (Table 5).

Under typical reaction conditions ($ZnL^{APIP}OAc$/TBAI at 70 °C), we obtained a low yield of cyclohexene carbonate (Table 5, entry 1). By increasing the temperature to 100 °C, the yield improved (Table 5, entry 2). Having employed TBAB as a co-catalyst and increased the amount of the catalyst and co-catalyst, cyclohexene carbonate was afforded in a high yield (Table 5, entry 4). This is attributed to the larger size of the iodide compared with bromide, which may prove unfavourable in the nucleophilic attack and ring-opening of a strictly hindered cyclohexene oxide.[95] Using tetrabutylammonium chloride (TBAC) as a co-catalyst did not improve the cyclohexene carbonate yield much, attributed to the poor leaving ability of the chloride anion, and to its stronger interaction with the tetrabutylammonium cation compared to bromide and iodide anions[96] (Table 5, entry 5). Then we tried to evaluate the efficiency of $ZnL^{APIP}I$ as a one-component catalyst in cyclohexene carbonate synthesis; however, the yield was only moderate at 22% (Table 5, entry 6).

Using TBAB as a co-catalyst at 70 °C, the yield of cyclohexene carbonate increased to 60%, and with further increase in temperature to 100 °C, the yield improved to 76% (Table 5, entry 8). Due to the hindrance of cyclohexene oxide as explained above and the larger size of iodide, we employed other Zn-based catalysts bearing bromide and chloride as axial ligands. The yield of cyclohexene carbonate was increased to 81% and 90%, as expected, when $ZnL^{APIP}Br$ and $ZnL^{APIP}Cl$ were utilized respectively.

We observed that hindered zinc complexes ($ZnL^{APIP}X$, X = Cl, Br, I) permitted the homopolymerization of cyclohexene epoxides to polyether. Gel permeation chromatography established that a low molecular weight of polymer is formed (Table 5, entries 6–11) (Fig. S3, ESI†).[96] The polyether was also identified by ^{1}H NMR analysis (Fig. S4, ESI†). That is, homo-polymerization of epoxides requires a site on zinc for epoxide binding. Indeed, halide derivative zinc complexes were found to be the most active to leave a site on zinc for homopolymerization of epoxides. On the other hand, a small substituent (*e.g.*, OAc) allows for CO_2 insertion to provide a carbonate intermediate.[97]

For sure, in the absence of steric inhibition, CO_2 insertion is more facile than epoxide ring-opening.[98] We also found that not only the conversion of cyclohexene oxide decreased to 55% when we utilize TBAB without any Zn-based catalyst, but also the amount of undesired polyether increased (Table 5, entry 11 and Fig. S3, ESI†).

In all cases, the *cis*-isomer of cyclohexene carbonate was the only product, in agreement with a mechanism in which an external nucleophilic anion displaces the metal-bound carbonate intermediate.[96,99]

Conclusions

Facile one-pot synthesis of new zinc complexes of an *o*-aminophenolate–iminopyridine hybrid ligand bearing different axial anions is presented to perform as efficient catalysts for CO_2 fixation into valuable compounds of cyclic carbonates.

X-ray crystallography analysis revealed that the zinc complexes exist as distorted square-pyramid Zn^{II} structures ($ZnL^{APIP}X$, X = OAc, Br, I) with an N_3O coordination environment at the equatorial region and a mono-dentate X ligand in the axial positions. By tailoring the nature of the axial ligand, the resulting complexes were studied to perform as binary and bifunctional catalysts for the coupling reaction of carbon dioxide (CO_2) with epoxides, leading to the formation of cyclic carbonates.

Under solvent free conditions, $ZnL^{APIP}OAc$ in combination with TBAI or TBAB was found to be a versatile catalyst to convert different epoxides including cyclohexene oxide to their corresponding cyclic carbonates in high yield and excellent selectivity, while $ZnL^{APIP}I$ as a one component catalyst could afford a high yield of cyclic carbonates with no addition of onium salts as the co-catalyst.

Experimental section

General information

All chemicals were purchased from Merck and Aldrich companies and used as received. Manipulations were performed under

aerobic conditions. 3,5-DTBQ (3,5-di-*tert*-butylcyclohexa-3,5-diene-1,2-dione) was synthesized according to a modified literature procedure.[100] FT-IR spectra were recorded in the solid state on a FT-IR Bruker Vector 22 spectrophotometer in the 400–4000 cm^{-1} range. NMR spectra were recorded at 400 MHz on a Bruker DRX spectrometer. The chemical shifts were referred to TMS using the residual signals from the solvent. Mass spectra (positive ion) were obtained on a Bruker Microflex LT MALDI-TOF MS instrument. Elemental analyses were carried out on Elementar Vario EL III.

X-ray structure determination

Brown crystals of $ZnL^{APIP}OAc$ complex suitable for the X-ray diffraction experiment were obtained from the methanol solution. $ZnL^{APIP}Br$ and $ZnL^{APIP}I$ complexes were crystallized from the CH_3CN–CH_2Cl_2 solution. For all compounds, the X-ray data were collected with an Oxford Sapphire CCD diffractometer using MoKα radiation λ = 0.71073 Å, at 293(2) K, by the ω–2θ method. Structures have been solved by direct methods and refined with the full-matrix least-squares method on F^2 with the use of the SHELX2014[101] program package. The analytical absorption correction was applied (RED171 package of programs[102] Oxford Diffraction, 2000) (Table 1). No extinction correction was applied. Hydrogen atoms were located from the electron density maps and their positions were constrained in the refinement.

Gel permeation chromatography (GPC) analyses were carried out at 40 °C using a Waters Breeze system equipped with a 1515 Refractive index detector. The samples were filtered before analysis. Tetrahydrofuran was used as the eluent.

After the catalytic test, the reaction products were analysed by means of ^{1}H NMR and ^{13}C NMR, FT-IR, and GPC.

The samples of reaction mixture for analysis by ^{1}H NMR were prepared by adding 2 mL of deuterated chloroform to the reaction mixture while stirring to dissolve the reagents, products and the catalyst. An aliquot of 50 μL of the obtained solution was diluted with 1 mL of $CDCl_3$ and analysed (cyclohexene oxide (δ = 3.1 ppm), carbonate linkages of poly (cyclohexene carbonate) (broad signal at δ = 4.65 ppm), polyether linkages of homo-polymerization (broad signal at δ = 3.45 ppm), *trans*-cyclohexene carbonate (δ = 4.0 ppm), and *cis*-cyclohexene carbonate (δ = 4.64 ppm)). The cyclic carbonate samples for FT-IR analysis were prepared by placing a small drop of isolated products diluted with CH_2Cl_2 on a KBr plate. The distinctive absorption band at 1793–1804 cm^{-1} is observed for the cyclic carbonate.[96]

Synthesis of $ZnL^{APIP}X$ (X = OAc, Cl, Br, I)

$ZnL^{APIP}X$ (X = OAc, Cl, Br, I) complexes were synthesized by the following one-pot reaction method. Firstly, to a solution of 3,5-DTBQ (0.22 g, 1 mmol) in acetonitrile (4 mL) was added 2-aminobenzyl amine (0.122 g, 1 mmol), and the reaction solution was stirred for 30 min at room temperature in the presence of air. After 30 minutes, it afforded a yellow precipitate (HL^{AP}). To a stirred suspension of HL^{AP} in acetonitrile was added pyridine-2-carboxaldehyde (0.096 mL, 1 mmol). For synthesis of different zinc complexes, various zinc precursors of Zn $(OAc)_2{\cdot}2H_2O$ (0.219 g, 1 mmol), $ZnCl_2$ (0.136 g, 1 mmol), $ZnBr_2$ (0.225, 1 mmol) and ZnI_2 (0.319, 1 mmol) were added to the reaction mixture immediately. Then, 2 equivalents of NEt_3 and 10 mL CH_3CN was added to induce the precipitation of the $ZnL^{APIP}OAc$, $ZnL^{APIP}Cl$, $ZnL^{APIP}Br$ and $ZnL^{APIP}I$ complexes after 2 h of stirring, respectively. Finally, the precipitate was filtrated and crystallized in dichloromethane/acetonitrile for further purification.

$ZnL^{APIP}OAc$

The filtrate was left undisturbed to afford dark brown microcrystals by evaporation from dichloromethane/acetonitrile solution (0.382 g, 70% yield). X-ray quality dark brown single crystals were grown from the methanol solution of the complex. ν max(KBr)/cm^{-1}: 3415 (O–H), 2946 (C–H), 1606 (C═O), 1593 (C═C), 1469 (C═N), 740 (═C–H bending) (Fig. S5, ESI†). ^{1}H NMR (400 MHz, DMSO-d_6) δ 9.09 (s, 1H), 9.00 (s, 1H), 8.93 (d, J = 4.90 Hz, 1H), 8.39 (td, J = 7.72, 1.65 Hz, 1H), 8.18 (d, J = 7.64 Hz, 1H), 8.06–7.97 (m, 2H), 7.76–7.70 (m, 1H), 7.65–7.61 (m, 2H), 7.41 (d, J = 2.33 Hz, 1H), 7.08 (d, J = 2.35 Hz, 1H), 1.59 (s, 3H), 1.45 (s, 9H), 1.29 (s, 9H) (Fig. S6, ESI†). ^{13}C NMR (100 MHz, $(CD_3)_2SO$): δ 29.8, 30.0, 32.1, 32.2, 34.4, 35.5, 109.7, 121.03, 124.5, 128.9, 129.2, 129.6, 129.7, 132.0, 132.3, 133.5, 135.5, 138.5, 141.9, 145.0, 147.4, 149.9, 153.08, 161.1, 162.7 (Fig. S7, ESI†). Elemental analysis: calculated: C, 64.74; H, 6.37; N, 7.81. Found: C, 64.95; H, 6.81; N, 7.58.

$ZnL^{APIP}Cl$

The filtrate was left undisturbed to afford dark brown microcrystals by evaporation from dichloromethane/acetonitrile solution (0.384 g, 75% yield). ν max(KBr)/cm^{-1}: 2948 (C–H), 1594 (C═C), 1470 (C═N), 745 (═C–H bending) (Fig. S8, ESI†). ^{1}H NMR (400 MHz, DMSO-d_6) δ 9.16 (s, 1H), 9.04 (s, 1H), 8.89 (d, J = 4.88 Hz, 1H), 8.44 (td, J = 7.73, 1.62 Hz, 1H), 8.23 (d, J = 7.65 Hz, 1H), 8.08 (dd, J = 8.32, 5.55 Hz, 1H), 8.03 (dd, J = 5.88, 3.45 Hz, 1H), 7.82 (dd, J = 5.86, 3.36 Hz, 1H), 7.71–7.63 (m, 2H), 7.45 (d, J = 2.31 Hz, 1H), 7.10 (d, J = 2.33 Hz, 1H), 1.46 (s, 9H), 1.30 (s, 9H) (Fig. S9, ESI†). ^{13}C NMR (100 MHz, $(CD_3)_2SO$) δ 29.8, 31.1, 32.1, 34.4, 35.5, 109.8, 121.2, 124.7, 128.8, 129.6, 130.0, 130.1, 132.1, 133.8, 135.7, 138.6, 142.2, 144.2, 147.35, 149.5, 153.0, 160.5, 162.60 (Fig. S10, ESI†). MALDI-MS m/z: 512.987 (Fig. S11, ESI†). Elemental analysis, calculated: C, 63.17; H, 5.89; N, 8.19. Found: C, 63.28; H, 5.49; N, 8.55.

$ZnL^{APIP}Br$

The filtrate was left undisturbed to afford dark brown microcrystals by evaporation from dichloromethane/acetonitrile solution (0.418 g, 75% yield). ν max(KBr)/cm^{-1}: 2948 (C–H), 1594 (C═C), 1470 (C═N), 745 (═C–H bending) (Fig. S12, ESI†). ^{1}H NMR (400 MHz, DMSO-d_6) δ 9.20 (s, 1H), 9.06 (s, 1H), 8.89 (d, J = 4.87 Hz, 1H), 8.45 (t, J = 7.72 Hz, 1H), 8.24 (d, J = 7.65 Hz, 1H), 8.09 (dd, J = 2.76, 1.15 Hz, 1H), 8.04 (dd, J = 5.89, 3.43 Hz, 1H), 7.87–7.82 (m, 1H), 7.71–7.65 (m, 2H), 7.47 (d, J = 2.30 Hz, 1H), 7.12 (d, J = 2.32 Hz, 1H), 1.47 (s, 9H), 1.30 (s, 9H) (Fig. S13, ESI†). ^{13}C NMR (100 MHz, $(CD_3)_2SO$) δ 29.8, 32.10, 34.4, 35.55, 109.9, 121.2, 124.8, 128.7, 129.8, 130.1, 130.2, 132.0, 132.3,

134.0, 135.8, 138.7, 142.38, 144.0, 147.2, 149.5, 153.4, 160.7, 162.3 (Fig. S14, ESI†). MALDI-MS *m*/*z*: 557.146 (Fig. S15, ESI†). Elemental analysis: C, 58.13; H, 5.42; N, 7.53. Found: C, 58.28; H, 5.47; N, 7.68.

$ZnL^{APIP}I$

The filtrate was left undisturbed to afford dark brown microcrystals by evaporation from dichloromethane/acetonitrile solution (0.483 g, 80% yield). ν max(KBr)/cm^{-1}: 2948 (C–H), 1594 (C═C), 1471 (C═N), 745 (═C–H bending) (Fig. S16, ESI†). ^{1}H NMR (400 MHz, DMSO-d_6) δ 9.29 (s, 1H), 9.14 (s, 1H), 8.86 (d, J = 4.85 Hz, 1H), 8.50 (td, J = 7.74, 1.57 Hz, 1H), 8.28 (d, J = 7.65 Hz, 1H), 8.17–8.11 (m, 1H), 8.11–8.06 (m, 1H), 7.93–7.85 (m, 1H), 7.76–7.66 (m, 2H), 7.52 (d, J = 2.26 Hz, 1H), 7.18 (d, J = 2.27 Hz, 1H), 1.51 (s, 9H), 1.31 (s, 9H) (Fig. S17, ESI†). ^{13}C NMR (100 MHz, $(CD_3)_2SO$) 29.9, 32.0, 34.5, 35.58, 110.2, 121.3, 125.1, 128.4, 130.1, 130.4, 130.6, 132.0, 132.6, 134.7, 136.5, 138.8, 142.8, 143.9, 147.23, 149.4, 154.4, 161.5, 161.8 (Fig. S18, ESI†). MALDI-MS *m*/*z*: 603.173 (Fig. S19, ESI†). Elemental analysis, calculated: C, 53.62; H, 5.00; N, 6.95; found: C, 53.85; H, 5.56; N, 6.66.

Typical experimental procedure for cyclic carbonate synthesis using $ZnL^{APIP}I$ as the catalyst

The coupling reactions were carried out in a 40 mL stainless steel autoclave equipped with a magnetic stir bar. In a typical reaction, the reactor was charged with an appropriate amount of catalyst and epoxide. After the reactor was pressurized with CO_2 to a desired pressure, the reaction mixture was heated to the desired temperature (100 °C) while stirring at about 800 rpm. Following the reaction, the reactor was cooled to ambient temperature, and the unreacted CO_2 was slowly released. The yield was obtained by GC using biphenyl as the internal standard.

Typical experimental procedure for cyclic carbonate synthesis using $ZnL^{APIP}OAc$ as the catalyst

The coupling reactions were carried out in a 40 mL stainless steel autoclave equipped with a magnetic stir bar. In a typical reaction, the reactor was charged with an appropriate amount of catalyst, epoxide and co-catalyst. After the reactor was pressurized with CO_2 to a desired pressure, the reaction mixture was heated while stirring at about 800 rpm. Following the reaction, the reactor was cooled to ambient temperature, and the unreacted CO_2 was slowly released. The yield was also obtained by GC using biphenyl as the internal standard. The resulting product was isolated using column chromatography and then identified by ^{1}H NMR, ^{13}C NMR, and FT-IR spectroscopy (Fig. S20, ESI†).

Acknowledgements

E. S. acknowledges the support by the Institute for Advanced Studies in Basic Sciences (IASBS). She gratefully thanks Prof. Aiwen Lei's collaboration for providing access to the GPC facility and Prof. Tim Storr's collaboration for performing MALDI-MS analyses.

References

1 D. J. Darensbourg, *Inorg. Chem.*, 2010, **49**, 10765–10780.
2 D. Tian, B. Liu, Q. Gan, H. Li and D. J. Darensbourg, *ACS Catal.*, 2012, **2**, 2029–2035.
3 A.-A. G. Shaikh and S. Sivaram, *Chem. Rev.*, 1996, **96**, 951–976.
4 S. H. Kim and S. H. Hong, *ACS Catal.*, 2014, **4**, 3630–3636.
5 O. Martin, M. Hammes, S. Mitchell and J. Pérez-Ramírez, *Energy Environ. Sci.*, 2014, **7**, 3640–3650.
6 G. Fiorani, W. Guo and A. W. Kleij, *Green Chem.*, 2015, **17**, 1375–1389.
7 S. Schenk, J. Notni, U. Kohn, K. Wermann and E. Anders, *Dalton Trans.*, 2006, 4191–4206.
8 M. Mondal, S. Khanra, O. Tiwari, K. Gayen and G. Halder, *Environ. Prog. Sustainable Energy*, 2016, **35**, 1605–1615.
9 T. Ema, Y. Miyazaki, S. Koyama, Y. Yano and T. Sakai, *Chem. Commun.*, 2012, **48**, 4489–4491.
10 M. Peters, B. Köhler, W. Kuckshinrichs, W. Leitner, P. Markewitz and T. E. Müller, *ChemSusChem*, 2011, **4**, 1216–1240.
11 Q. Liu, L. Wu, R. Jackstell and M. Beller, *Nat. Commun.*, 2015, **6**, 5933.
12 F.-T. Tsai, Y. Wang and D. J. Darensbourg, *J. Am. Chem. Soc.*, 2016, **138**, 4626–4633.
13 B. Yu and L. N. He, *ChemSusChem*, 2015, **8**, 52–62.
14 D. J. Darensbourg and S. J. Wilson, *J. Am. Chem. Soc.*, 2011, **133**, 18610–18613.
15 J. H. Clements, *Ind. Eng. Chem. Res.*, 2003, **42**, 663–674.
16 T. Sakakura and K. Kohno, *Chem. Commun.*, 2009, 1312–1330.
17 B. Schäffner, J. Holz, S. P. Verevkin and A. Börner, *ChemSusChem*, 2008, **1**, 249–253.
18 C.-X. Miao, J.-Q. Wang, Y. Wu, Y. Du and L.-N. He, *ChemSusChem*, 2008, **1**, 236–241.
19 J. Bayardon, J. Holz, B. Schäffner, V. Andrushko, S. Verevkin, A. Preetz and A. Börner, *Angew. Chem., Int. Ed.*, 2007, **46**, 5971–5974.
20 P. Tundo and M. Selva, *Acc. Chem. Res.*, 2002, **35**, 706–716.
21 B. Schäffner, F. Schäffner, S. P. Verevkin and A. Börner, *Chem. Rev.*, 2010, **110**, 4554–4581.
22 V. Etacheri, R. Marom, R. Elazari, G. Salitra and D. Aurbach, *Energy Environ. Sci.*, 2011, **4**, 3243–3262.
23 B. Scrosati, J. Hassoun and Y.-K. Sun, *Energy Environ. Sci.*, 2011, **4**, 3287–3295.
24 X. Xiaoding and J. A. Moulijn, *Energy Fuels*, 1996, **10**, 305–325.
25 M. Bahr and R. Mulhaupt, *Green Chem.*, 2012, **14**, 483–489.
26 V. Besse, F. Camara, C. Voirin, R. Auvergne, S. Caillol and B. Boutevin, *Polym. Chem.*, 2013, **4**, 4545–4561.
27 M. Fleischer, H. Blattmann and R. Mulhaupt, *Green Chem.*, 2013, **15**, 934–942.

28 C. Beattie, M. North, P. Villuendas and C. Young, *J. Org. Chem.*, 2013, **78**, 419–426.
29 V. Laserna, G. Fiorani, C. J. Whiteoak, E. Martin, E. Escudero-Adán and A. W. Kleij, *Angew. Chem., Int. Ed.*, 2014, **53**, 10416–10419.
30 M. North, R. Pasquale and C. Young, *Green Chem.*, 2010, **12**, 1514–1539.
31 X.-B. Lu and D. J. Darensbourg, *Chem. Soc. Rev.*, 2012, **41**, 1462–1484.
32 C. Maeda, J. Shimonishi, R. Miyazaki, J. y. Hasegawa and T. Ema, *Chem. – Eur. J.*, 2016, **22**, 6556–6563.
33 Y. Ren and J.-J. Shim, *ChemCatChem*, 2013, **5**, 1344–1349.
34 C.-Y. Li, D.-C. Liu and B.-T. Ko, *Dalton Trans.*, 2013, **42**, 11488–11496.
35 R. Luo, X. Zhou, S. Chen, Y. Li, L. Zhou and H. Ji, *Green Chem.*, 2014, **16**, 1496–1506.
36 C. J. Whiteoak, N. Kielland, V. Laserna, E. C. Escudero-Adán, E. Martin and A. W. Kleij, *J. Am. Chem. Soc.*, 2013, **135**, 1228–1231.
37 P. Gao, Z. Zhao, L. Chen, D. Yuan and Y. Yao, *Organometallics*, 2016, **35**, 1707–1712.
38 M. A. Fuchs, C. Altesleben, T. A. Zevaco and E. Dinjus, *Eur. J. Inorg. Chem.*, 2013, 4541–4545.
39 J. A. Castro-Osma, M. North and X. Wu, *Chem. – Eur. J.*, 2016, **22**, 2100–2107.
40 M. Cozzolino, T. Rosen, I. Goldberg, M. Mazzeo and M. Lamberti, *ChemSusChem*, 2017, **10**, 1217–1223.
41 D. J. Darensbourg, J. C. Yarbrough, C. Ortiz and C. C. Fang, *J. Am. Chem. Soc.*, 2003, **125**, 7586–7591.
42 J. A. Castro-Osma, K. J. Lamb and M. North, *ACS Catal.*, 2016, **6**, 5012–5025.
43 P. Yan and H. Jing, *Adv. Synth. Catal.*, 2009, **351**, 1325–1332.
44 M. A. Fuchs, S. Staudt, C. Altesleben, O. Walter, T. A. Zevaco and E. Dinjus, *Dalton Trans.*, 2014, **43**, 2344–2347.
45 A. Buonerba, A. De Nisi, A. Grassi, S. Milione, C. Capacchione, S. Vagin and B. Rieger, *Catal. Sci. Technol.*, 2015, **5**, 118–123.
46 F. Della Monica, S. V. Vummaleti, A. Buonerba, A. D. Nisi, M. Monari, S. Milione, A. Grassi, L. Cavallo and C. Capacchione, *Adv. Synth. Catal.*, 2016, **358**, 3231–3243.
47 D. Alhashmialameer, J. Collins, K. Hattenhauer and F. M. Kerton, *Catal. Sci. Technol.*, 2016, **6**, 5364–5373.
48 D. Bai, S. Duan, L. Hai and H. Jing, *ChemCatChem*, 2012, **4**, 1752–1758.
49 A. Chen, Y. Zhang, J. Chen, L. Chen and Y. Yu, *J. Mater. Chem. A*, 2015, **3**, 9807–9816.
50 C. Maeda, T. Taniguchi, K. Ogawa and T. Ema, *Angew. Chem.*, 2015, **127**, 136–140.
51 A. Decortes, A. M. Castilla and A. W. Kleij, *Angew. Chem., Int. Ed.*, 2010, **49**, 9822–9837.
52 R. L. Paddock and S. T. Nguyen, *Chem. Commun.*, 2004, 1622–1623.
53 R. L. Paddock and S. T. Nguyen, *J. Am. Chem. Soc.*, 2001, **123**, 11498–11499.
54 T. Chang, H. Jing, L. Jin and W. Qiu, *J. Mol. Catal. A: Chem.*, 2007, **264**, 241–247.
55 X. Zhang, Y.-B. Jia, X.-B. Lu, B. Li, H. Wang and L.-C. Sun, *Tetrahedron Lett.*, 2008, **49**, 6589–6592.
56 Y. Ren, J. Chen, C. Qi and H. Jiang, *ChemCatChem*, 2015, **7**, 1535–1538.
57 A. Decortes, M. Martinez Belmonte, J. Benet-Buchholz and A. W. Kleij, *Chem. Commun.*, 2010, **46**, 4580–4582.
58 C. Martin, C. Whiteoak, E. Martin, M. M. Belmonte, E. Escudero-Adán and A. Kleij, *Catal. Sci. Technol.*, 2014, **4**, 1615–1621.
59 W.-M. Ren, Y. Liu and X.-B. Lu, *J. Org. Chem.*, 2014, **79**, 9771–9777.
60 A. Decortes and A. W. Kleij, *ChemCatChem*, 2011, **3**, 831–834.
61 D. J. Darensbourg and M. W. Holtcamp, *Coord. Chem. Rev.*, 1996, **153**, 155–174.
62 H. Büttner, J. Steinbauer and T. Werner, *ChemSusChem*, 2015, **8**, 2655–2669.
63 H. Büttner, K. Lau, A. Spannenberg and T. Werner, *ChemCatChem*, 2015, **7**, 459–467.
64 Y. Tsutsumi, K. Yamakawa, M. Yoshida, T. Ema and T. Sakai, *Org. Lett.*, 2010, **12**, 5728–5731.
65 S. Liu, N. Suematsu, K. Maruoka and S. Shirakawa, *Green Chem.*, 2016, **18**, 4611–4615.
66 V. B. Saptal and B. M. Bhanage, *ChemCatChem*, 2016, **8**, 244–250.
67 X. Wang, Y. Zhou, Z. Guo, G. Chen, J. Li, Y. Shi, Y. Liu and J. Wang, *Chem. Sci.*, 2015, **6**, 6916–6924.
68 T. Werner, N. Tenhumberg and H. Büttner, *ChemCatChem*, 2014, **6**, 3493–3500.
69 D. Xing, B. Lu, H. Wang, J. Zhao and Q. Cai, *New J. Chem.*, 2017, **41**, 387–392.
70 T. Chang, L. Jin and H. Jing, *ChemCatChem*, 2009, **1**, 379–383.
71 E. K. Noh, S. J. Na, S.-W. Kim and B. Y. Lee, *J. Am. Chem. Soc.*, 2007, **129**, 8082–8083.
72 W.-M. Ren, X. Zhang, Y. Liu, J.-F. Li, H. Wang and X.-B. Lu, *Macromolecules*, 2010, **43**, 1396–1402.
73 J. Melendez, M. North and P. Villuendas, *Chem. Commun.*, 2009, 2577–2579.
74 J. Melendez, M. North, P. Villuendas and C. Young, *Dalton Trans.*, 2011, **40**, 3885–3902.
75 D. Tian, B. Liu, L. Zhang, X. Wang, W. Zhang, L. Han and D.-W. Park, *J. Ind. Eng. Chem.*, 2012, **18**, 1332–1338.
76 Y. Wang, J. L. DuBois, B. Hedman, K. O. Hodgson and T. Stack, *Science*, 1998, **279**, 537–540.
77 P. Chaudhuri, M. Hess, J. Müller, K. Hildenbrand, E. Bill, T. Weyhermüller and K. Wieghardt, *J. Am. Chem. Soc.*, 1999, **121**, 9599–9610.
78 P. Chaudhuri, M. Hess, T. Weyhermüller and K. Wieghardt, *Angew. Chem., Int. Ed.*, 1999, **38**, 1095–1098.
79 S. E. Balaghi, E. Safaei, L. Chiang, E. W. Wong, D. Savard, R. M. Clarke and T. Storr, *Dalton Trans.*, 2013, **42**, 6829–6839.
80 Z. Alaji, E. Safaei, L. Chiang, R. M. Clarke, C. Mu and T. Storr, *Eur. J. Inorg. Chem.*, 2014, 6066–6074.
81 X.-B. Lu, B. Liang, Y.-J. Zhang, Y.-Z. Tian, Y.-M. Wang, C.-X. Bai, H. Wang and R. Zhang, *J. Am. Chem. Soc.*, 2004, **126**, 3732–3733.

82 X. B. Lu and Y. Wang, *Angew. Chem., Int. Ed.*, 2004, **43**, 3574–3577.
83 H. Jing, S. K. Edulji, J. M. Gibbs, C. L. Stern, H. Zhou and S. T. Nguyen, *Inorg. Chem.*, 2004, **43**, 4315–4327.
84 D. J. Darensbourg and J. C. Yarbrough, *J. Am. Chem. Soc.*, 2002, **124**, 6335–6342.
85 W. Clegg, R. W. Harrington, M. North and R. Pasquale, *Chem. – Eur. J.*, 2010, **16**, 6828–6843.
86 J. Melèndez, M. North and P. Villuendas, *Chem. Commun.*, 2009, 2577–2579.
87 J. E. Dengler, M. W. Lehenmeier, S. Klaus, C. E. Anderson, E. Herdtweck and B. Rieger, *Eur. J. Inorg. Chem.*, 2011, 336–343.
88 M. V. Escárcega-Bobadilla, M. Martínez Belmonte, E. Martin, E. C. Escudero-Adán and A. W. Kleij, *Chem. – Eur. J.*, 2013, **19**, 2641–2648.
89 C. K. A. Gregson, V. C. Gibson, N. J. Long, E. L. Marshall, P. J. Oxford and A. J. P. White, *J. Am. Chem. Soc.*, 2006, **128**, 7410–7411.
90 V. Lyaskovskyy and B. de Bruin, *ACS Catal.*, 2012, **2**, 270–279.
91 M. North and R. Pasquale, *Angew. Chem., Int. Ed.*, 2009, **121**, 2990–2992.
92 S. Supasitmongkol and P. Styring, *Catal. Sci. Technol.*, 2014, **4**, 1622–1630.
93 N. Aoyagi, Y. Furusho and T. Endo, *J. Polym. Sci., Part A: Polym. Chem.*, 2013, **51**, 1230–1242.
94 M. Taherimehr, A. Decortes, S. M. Al-Amsyar, W. Lueangchaichaweng, C. J. Whiteoak, E. C. Escudero-Adán, A. W. Kleij and P. P. Pescarmona, *Catal. Sci. Technol.*, 2012, **2**, 2231–2237.
95 C. J. Whiteoak, E. Martin, M. M. Belmonte, J. Benet-Buchholz and A. W. Kleij, *Adv. Synth. Catal.*, 2012, **354**, 469–476.
96 M. Taherimehr, S. M. Al-Amsyar, C. J. Whiteoak, A. W. Kleij and P. P. Pescarmona, *Green Chem.*, 2013, **15**, 3083–3090.
97 D. J. Darensbourg, S. J. Lewis, J. L. Rodgers and J. C. Yarbrough, *Inorg. Chem.*, 2003, **42**, 581–589.
98 D. J. Darensbourg, M. W. Holtcamp, G. E. Struck, M. S. Zimmer, S. A. Niezgoda, P. Rainey, J. B. Robertson, J. D. Draper and J. H. Reibenspies, *J. Am. Chem. Soc.*, 1999, **121**, 107–116.
99 C. J. Whiteoak, E. Martin, E. Escudero-Adán and A. W. Kleij, *Adv. Synth. Catal.*, 2013, **355**, 2233–2239.
100 T. Khomenko, O. Salomatina, S. Y. Kurbakova, I. Il'ina, K. Volcho, N. Komarova, D. Korchagina, N. Salakhutdinov and A. Tolstikov, *Russ. J. Org. Chem.*, 2006, **42**, 1653–1661.
101 G. M. Sheldrick, *Acta Crystallogr., Sect. A: Found. Crystallogr.*, 2008, **64**, 112–122.
102 R. O. CrysAlis Pro 171.38.43 program package, 2015.